

Electronic Supplementary Information for “Pyrophosphate Selective Fluorescent Chemosensors Based on Coumarin-DPA-Cu(II) Complexes”

Min Jung Kim,^a K. M. K. Swamy,^{a,b} Kyung Mi Lee,^a Arun R. Jagdale,^a Youngmee Kim,^a
Sung-Jin Kim,^a Kyung Ho Yoo^c and Juyoung Yoon^{*a,d}

^a Department of Chemistry and Nano Science, Ewha Womans University, Seoul 120-750, Korea. Fax:

+82-2-3277-3419; Tel: +82-2-3277-2400; E-mail: jyoony@ewha.ac.kr

^b Department of Pharmaceutical Chemistry, V. L. College of Pharmacy,

Raichur-584 103, India.

^c Life Sciences Research Division, Korea Institute of Science and Technology, P.O. Box 131,

Cheongryang, Seoul 130-650, Korea

^d Department of Bioinspired Science, Ewha Womans University, Seoul 120-750, Korea

Experimental Section	-----	S3 page
Figure S1.	Synthesis of 1 and 3 -----	S3 page
Figure S2.	Synthesis of 2 and 4 -----	S4 page
Figure S3.	Plot of fluorescence intensity changes of 1 (3 μ M) in the presence of PPI -----	S8 page
Figure S4.	Plot of fluorescence intensity changes of 2 (3 μ M) in the presence of PPI -----	S9 page
Figure S5.	Plot of fluorescence intensity changes of 1 (3 μ M) versus equivalents of PPI ---	S9 page
Figure S6.	Plot of fluorescence intensity changes of 2 (3 μ M) versus concentration of PPI --	S10 page
Figure S7.	Job's plot of the complexation between 1 and PPI -----	S10 page
Figure S8.	Job's plot of the complexation between 2 and PPI -----	S11 page
Figure S9.	Plot fluorescence changes of compound 3 (3 μ M) upon the addition of PPI, Pi, ATP, ADP, AMP, CH ₃ COO ⁻ , HSO ₄ ⁻ , F ⁻ , Cl ⁻ , Br ⁻ and I ⁻ (100equiv.) -----	S11 page
Figure S10.	Plot fluorescence changes of compound 4 (3 μ M) upon the addition of PPI, Pi, ATP, ADP, AMP, CH ₃ COO ⁻ , HSO ₄ ⁻ , F ⁻ , Cl ⁻ , Br ⁻ and I ⁻ (100equiv) -----	S12 page
Figure S11.	Portion ESI mass spectrum of 1 upon the addition of excess PPI (5 equiv.) ----	S12 page

Figure S12.	$^1\text{H-NMR}$ (CDCl_3 , 250 MHz) of compound 5 -----	S13 page
Figure S13.	$^{13}\text{C-NMR}$ (CDCl_3 , 250 MHz) of compound 5 -----	S13 page
Figure S14.	FAB mass spectrum of compound 5 -----	S14 page
Figure S15.	$^1\text{H-NMR}$ ($\text{DMSO-}d_6$, 250 MHz) of compound 7 -----	S14 page
Figure S16.	$^{13}\text{C-NMR}$ ($\text{DMSO-}d_6$, 250 MHz) of compound 7 -----	S15 page
Figure S17.	FAB mass spectrum of compound 7 -----	S15 page
Figure S18.	FAB mass spectrum of compound 1 -----	S16 page
Figure S19.	FAB mass spectrum of compound 3 -----	S16 page
Figure S20.	$^1\text{H-NMR}$ (D_2O , 250 MHz) of compound 3 -----	S17 page
Figure S21.	$^{13}\text{C-NMR}$ (D_2O , 250 MHz) of compound 3 -----	S17 page
Figure S22.	FAB mass spectrum of compound 2 -----	S18 page
Figure S23.	FAB mass spectrum of compound 4 -----	S18 page
Figure S24.	$^1\text{H-NMR}$ (D_2O , 250 MHz) of compound 4 -----	S19 page
Figure S25.	$^{13}\text{C-NMR}$ (D_2O , 250 MHz) of compound 4 -----	S19 page

Experimental Section

General methods. Unless otherwise noted, materials were obtained from commercial suppliers and were used without further purification. Flash chromatography was carried out on silica gel 60 (230-400 mesh ASTM; Merck). Thin layer chromatography (TLC) was carried out using Merck 60 F₂₅₄ plates with a thickness of 0.25 mm. Preparative TLC was performed using Merck 60 F₂₅₄ plates with a thickness of 1 mm.

Melting points were measured using a Büchi 530 melting point apparatus, and are uncorrected. ¹H NMR and ¹³C NMR spectra were recorded using Bruker 250 or Varian 500. Chemical shifts were expressed in ppm and coupling constants (*J*) in Hz. Mass spectra were obtained using a JMS-HX 110A/110A Tandem Mass Spectrometer (JEOL). UV absorption spectra were obtained on UVIKON 933 Double Beam UV/VIS Spectrometer. Fluorescence emission spectra were obtained using RF-5301/PC Spectrofluorophotometer (Shimadzu).

Synthesis

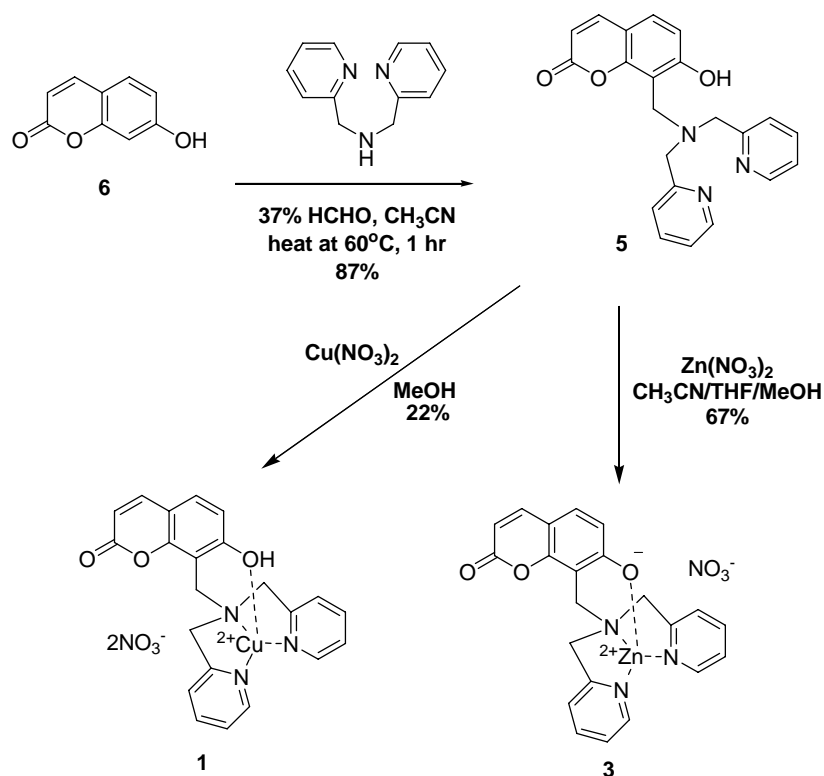


Figure-S1. Synthesis of **1** and **3**

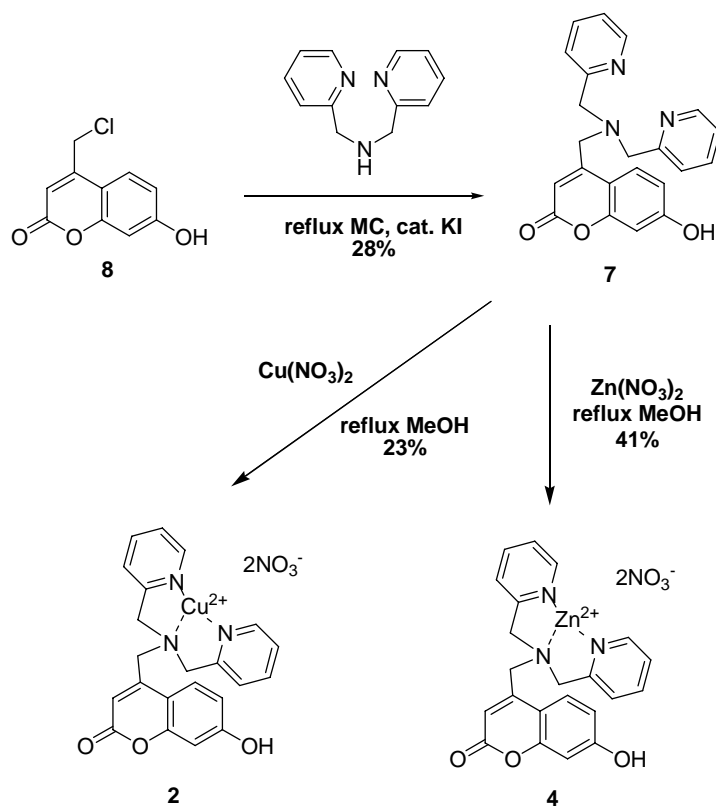


Figure-S2. Synthesis of **2** and **4**

Compound 5. To a solution of dipicolylamine (0.62 g, 3.08 mmol) in 30 mL of acetonitrile was added aqueous formaldehyde (37%) (0.27 mL, 3.08 mmol). After 0.5 h of heated at 60°C , the 7-hydroxycoumarin (0.50 g, 3.08 mmol) in 30 mL of acetonitrile was added. The duration of the reaction was 1 h, and the reaction was monitored by TLC. The solvent was removed under reduced pressure. The crude viscous orange colored oil was purified by silica column using ethyl acetate-methanol (98:2) as eluent to give light yellow solid **5** (1.0 g, 87 %); mp 144.5°C ; $^1\text{H NMR}$ (CDCl_3) δ 12.2 (hydroxy group, 1H), 8.56 (dq, 2H, $J = 4.1$ Hz, $J = 0.9$ Hz), 7.66 (td, 2H, $J = 7.7$ Hz, $J = 1.8$ Hz), 7.61 (d, 1H, $J = 0.5$ Hz), 7.35(d, 2H, $J = 7.8$ Hz), 7.28 (m, 1H), 7.18 (m, 2H), 6.87 (d, 1H, $J = 8.5$ Hz), 6.18 (d, 1H, $J = 9.4$ Hz), 4.01 (s,

2H), 3.91 (s, 4H); ^{13}C NMR (CDCl_3) δ 162.3, 161.4, 157.8, 153.9, 148.8, 144.3, 136.9, 128.2, 123.2, 122.4, 114.3, 111.4, 111.2, 110.4, 58.9, 47.7; HRMS(FAB) $m/z = 374.1501$ ($\text{M}+\text{H}$) $^+$, calc. for $\text{C}_{22}\text{H}_{20}\text{N}_3\text{O}_3 = 374.1505$, Elemental analysis(%) calc. for $\text{C}_{22}\text{H}_{19}\text{N}_3\text{O}_3$ (373.40): C 70.76, H 5.13, N 11.25; found C 70.28, H 5.24, N 11.19.

Compound 1. To a solution of **5** (100 mg, 0.27 mmol) in MeOH (6 ml) was added dropwise $\text{Cu}(\text{NO}_3)_2$ (0.54 mmol) in MeOH (2 ml). After stirring for 12 h at room temperature, the precipitate was filtered to give **1** (33.6 mg, 22 %) as a blue powder; mp 220.3 °C (decomposition), HRMS(FAB) $m/z = 498.0606$ [$\text{M}-\text{NO}_3^-$] $^+$, calc. for $\text{C}_{22}\text{H}_{19}\text{N}_4\text{O}_6\text{Cu} = 498.0601$, Elemental analysis(%) calc. for $\text{C}_{22}\text{H}_{19}\text{CuN}_5\text{O}_9$ (560.96): C 47.10, H 3.41, N 12.48; found C 46.89, H 3.37, N 12.25.

Compound 3. To a solution of **5** (100 mg, 0.27 mmol) in $\text{CH}_3\text{CN}-\text{THF}$ (5:1, 5 ml) was added dropwise $\text{Zn}(\text{NO}_3)_2$ (0.54 mmol) in MeOH (2 ml). After stirring for 30min at room temperature, the precipitate was filtered to give **3** (92.3 mg, 67%) as a yellowish light green powder; mp 214.37 °C (decomposition); ^1H NMR (D_2O) δ 8.45 (d, 2H, $J = 5.3$ Hz), 7.81 (t, 2H, $J = 7.8$ Hz), 7.72 (m, 1H), 7.40 (t, 2H, $J = 6.5$ Hz), 7.23 (d, 2H, $J = 7.9$ Hz), 7.07 (m, 1H), 6.40 (d, 1H, $J = 8.6$ Hz), 6.07 (d, 1H, $J = 9.4$ Hz), 4.23 (d, 2H, $J = 16.3$ Hz), 4.07 (d, 2H, $J = 16.2$ Hz), 3.75 (brs, 2H) ; ^{13}C NMR (D_2O) δ 164.6, 154.9, 153.5, 147.4, 146.8, 141.0, 130.4, 125.0, 124.0, 115.1, 111.6, 110.0, 109.1, 58.6, 47.1; HRMS(FAB) $m/z = 436.0642$ [$\text{M}-\text{NO}_3^-$] $^+$, calc. for $\text{C}_{22}\text{H}_{18}\text{N}_3\text{O}_3\text{Zn} = 436.0640$, Elemental analysis(%) calc. for $\text{C}_{22}\text{H}_{18}\text{N}_4\text{O}_6\text{Zn}$ (499.79): C 52.87, H 3.63, N 11.21; found C 52.62, H 3.62, N 11.36.

Compound 7. 4-Chloromethyl-7-methoxycoumarin (1g, 4.75 mmol) and dipicolylamine (1.89g, 9.49 mmol) were refluxed in methylene chloride (60 mL) for 14 h in the presence of a catalytic amount of KI. After cooling to ambient temperature, the solvent was evaporated and added dichloromethane (60 mL). The solids were filtered and dried in vacuum. The crude product (1.4g, 79%) was crystallized in aqueous ethanol to give **7** in 28 % yield (500 mg); mp 242.3 °C; ¹H NMR (DMSO-*d*₆) δ 10.6 (hydroxyl group, 1H), 8.50 (m, 2H), 7.77 (td, 2H, *J* = 7.6 Hz & 1.6 Hz), 7.64 (d, 1H, *J* = 8.7 Hz), 7.47 (d, 2H, *J* = 7.8 Hz), 7.26 (dd, 2H, *J* = 7.3 Hz & 4.9 Hz), 6.74 (d, 1H, *J* = 8.7 Hz & 2.3Hz), 6.67 (d, 1H, *J* = 2.2 Hz), 6.45 (s, 1H), 3.86 (s, 2H), 3.82 (s, 4H) ; ¹³C NMR (DMSO-*d*₆) δ 160.9, 160.4, 158.4, 154.9, 153.5, 148.9, 136.6, 126.3, 122.8, 122.3, 112.6, 110.6, 109.8, 102.1, 59.7, 54.1; HRMS(FAB) *m/z* = 374.1503 (M+H)⁺, calc. for C₂₂H₂₀N₃O₃ = 374.1505, Elemental analysis(%) calc. for C₂₂H₁₉N₃O₃ (373.40): C 70.76, H 5.13, N 11.25; found C 70.50, H 5.24, N 11.35.

Compound 2. To a solution of **7** (100 mg, 0.27 mmol) was refluxed in MeOH (30 ml) and was added dropwise Cu(NO₃)₂ (0.54mmol) in MeOH (2ml) for 12h. The precipitate was filtered to give **2** (35.2 mg, 23 %) as a dark blue powder; mp 234.1 °C (decomposition); HRMS(FAB) *m/z* = 498.0598 [M-NO₃]⁺, calc. for C₂₂H₁₉N₄O₆Cu = 498.0601, Elemental analysis(%) calc. for C₂₂H₁₉CuN₅O₉ (560.96): C 47.10, H 3.41, N 12.48; found C 46.90, H 3.27, N 12.12.

Compound 4. To a solution of **7** (100 mg, 0.27 mmol) was refluxed in MeOH (30 ml) and was added dropwise Zn(NO₃)₂ (0.54 mmol) in MeOH (2 ml) for 3h. The precipitate was filtered to give **4** (73.3 mg, 41 %) as a yellowish light green powder; mp 200°C (decomposition); ¹H NMR (D₂O) δ 8.57 (d, 2H, *J* = 5.1 Hz), 8.00 (t, 2H, *J* = 7.7 Hz), 7.55 (t,

2H, $J = 6.4$ Hz), 7.38 (d, 2H, $J = 7.9$ Hz), 7.06 (d, 1H, $J = 8.6$ Hz), 6.70 (m, 2H), 6.06 (s, 1H), 4.30 (d, 2H, $J = 16.4$), 3.99 (d, 2H, $J = 16.3$), 3.17 (s, 2H); ^{13}C NMR (D_2O) δ 164.0, 155.4, 154.3, 148.4, 148.0, 141.6, 126.5, 125.4, 125.2, 114.3, 103.6, 97.8, 56.2, 49.1 ; HRMS(FAB) $m/z = 499.0592$ $[\text{M}-\text{NO}_3]^{+}$, calc. for $\text{C}_{22}\text{H}_{19}\text{N}_4\text{O}_6\text{Zn} = 499.0596$, Elemental analysis(%) calc. for $\text{C}_{22}\text{H}_{19}\text{N}_5\text{O}_9\text{Zn}$ (562.8): C 46.95, H 3.40, N 12.44; found C 45.92, H 3.42, N 12.18.

Preparation of fluorometric anion titration solutions.

Stock solutions (10 mM) of the sodium salts of PPI, Pi, AMP, ADP and ATP in 20 mM HEPES (pH 7.4) were prepared. Stock solutions of host (0.6mM) were also prepared in distilled water. Test solutions were prepared by placing 3-30 μL of the probe stock solution into a test tube, adding an appropriate aliquot of each anion stock, and diluting the solution to 3mL with HEPES (0.02 M, pH 7.4).

X-ray data.

The X-ray diffraction data for two compounds were collected on a Bruker SMART APEX diffractometer equipped with a monochromator in the Mo Ka ($k = 0.71073$ Å) incident beam. Each crystal was mounted on a glass fiber. The CCD data were integrated and scaled using the Bruker-S SAINT software package, and the structure was solved and refined using SHELXTL V6.12. All hydrogen atoms were placed in the calculated positions. *Crystal data for 1* : $\text{C}_{44}\text{H}_{42}\text{Cu}_2\text{N}_{10}\text{O}_{20}$, $M = 1157.96$, Triclinic (P-1), $a = 8.4488(8)$ Å, $b = 8.4998(8)$ Å, $c = 17.5045(16)$ Å, $\alpha = 83.423(2)^\circ$, $\beta = 81.649(2)^\circ$, $\gamma = 79.468(2)^\circ$, $V = 1217.8(2)$ Å³, $Z = 1$, $\mu(\text{Mo-K}\alpha) = 0.964$ mm⁻¹, 6753 reflections measured, 4616 unique ($R_{\text{int}} = 0.0548$) which were used in all calculations, final $R = 0.0598$ ($R_w = 0.1697$) with reflections having intensities

greater than 2σ , GOF (F^2) = 1.009. Crystal data for **2** : $C_{22}H_{19}CuN_5O_9$, $M = 560.96$, Orthorhombic ($P2_12_12_1$), $a = 8.8036(10) \text{ \AA}$, $b = 13.0269(15) \text{ \AA}$, $c = 19.063(2) \text{ \AA}$, $V = 2186.2(4) \text{ \AA}^3$, $Z = 4$, $\mu(\text{Mo-K}\alpha) = 1.068 \text{ mm}^{-1}$, 12120 reflections measured, 4295 unique ($R_{\text{int}} = 0.0707$) which were used in all calculations, final $R = 0.0421$ ($R_w = 0.0698$) with reflections having intensities greater than 2σ , GOF (F^2) = 0.838. CCDC reference numbers 737519 for **1** and 737520 for **2**.

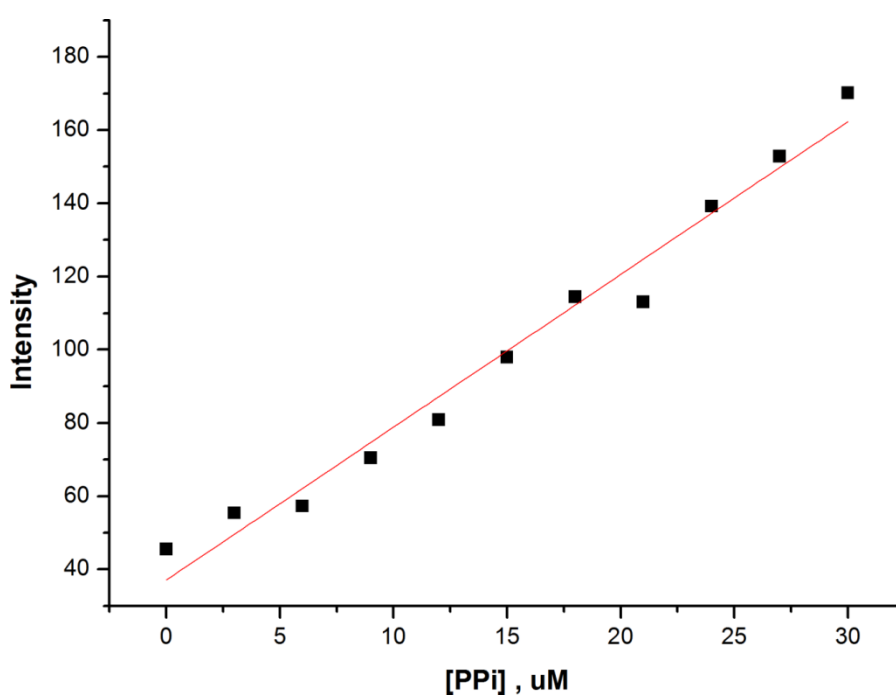


Figure-S3. Plot of fluorescence intensity changes of **1** ($3\mu\text{M}$) in the presence of PPI (3 to 30 μM) at pH 7.4 (20 mM HEPES) ($\lambda_{\text{ex}} = 366 \text{ nm}$, $\lambda_{\text{em}} 446 \text{ nm}$, Slit: 10 nm/10 nm).

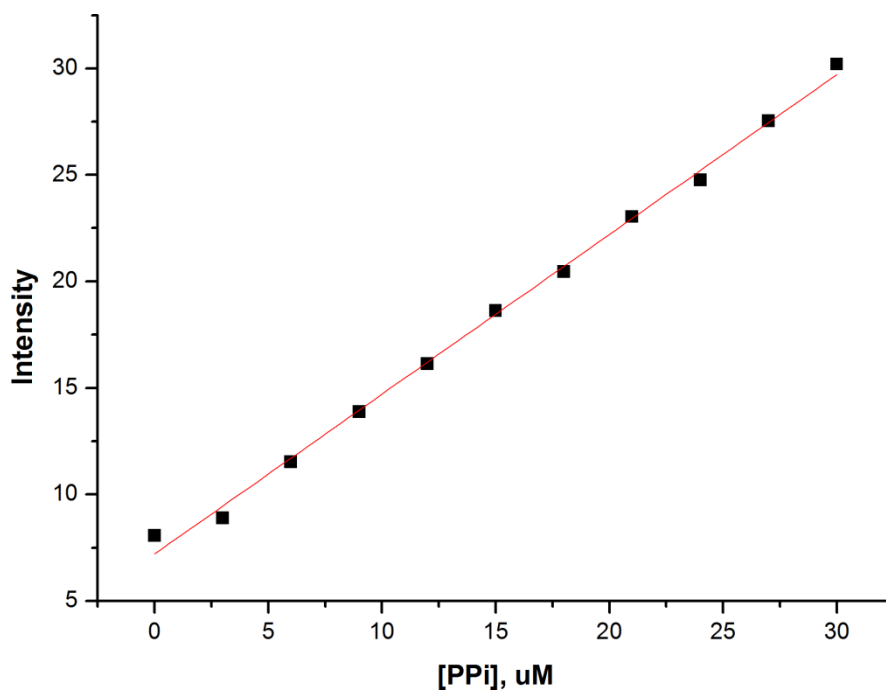


Figure-S4. Plot of fluorescence intensity changes of **2** ($3\mu\text{M}$) in the presence of PPI (3 to 30 μM) at pH 7.4 (20 mM HEPES) ($\lambda_{\text{ex}} = 393\text{ nm}$, $\lambda_{\text{em}} 472\text{ nm}$, Slit: 5 nm/5 nm).

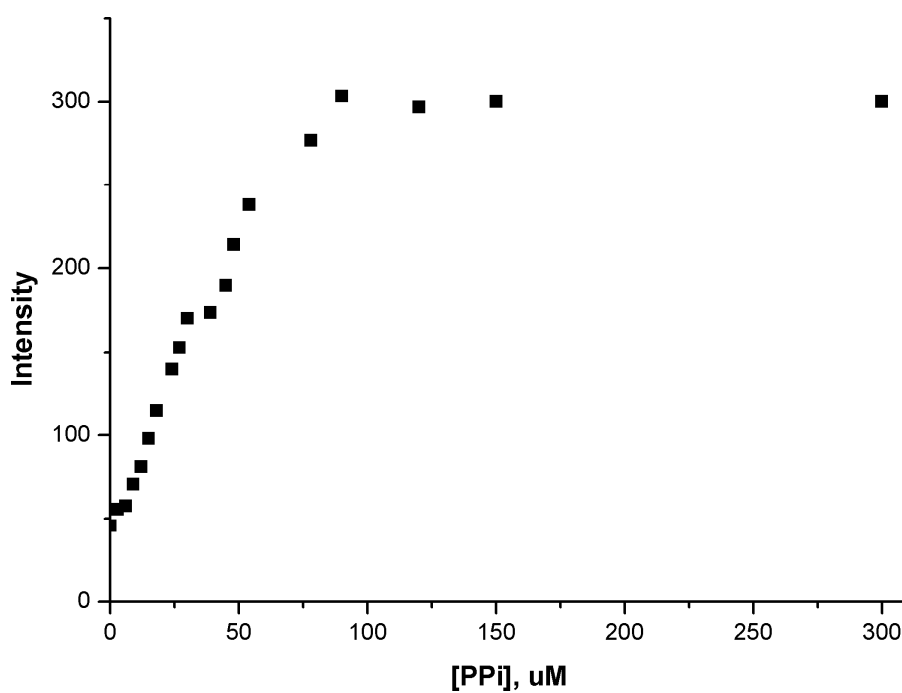


Figure-S5. Plot of fluorescence intensity changes of **1** ($3\mu\text{M}$) versus equivalents of PPI (at 446nm).

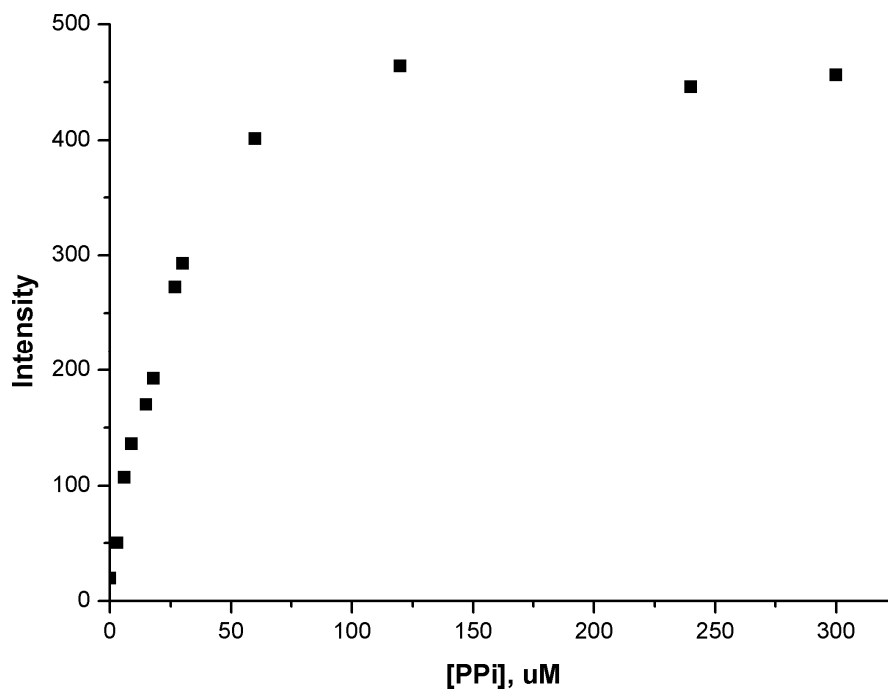


Figure-S6. Plot of fluorescence intensity changes of **2** (3 μM) versus concentration of PPI (at 475 nm).

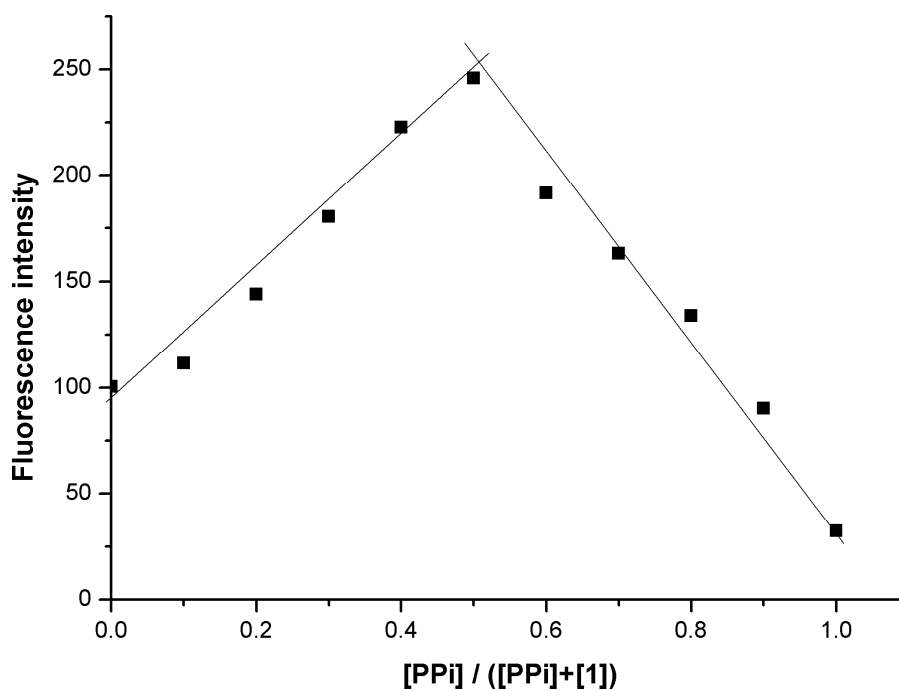


Figure-S7. Job's plot of the complexation between **1** and PPI in 20 mM HEPES solution at pH 7.4. Total concentration of **1** and PPI was kept constant at 3 μM.

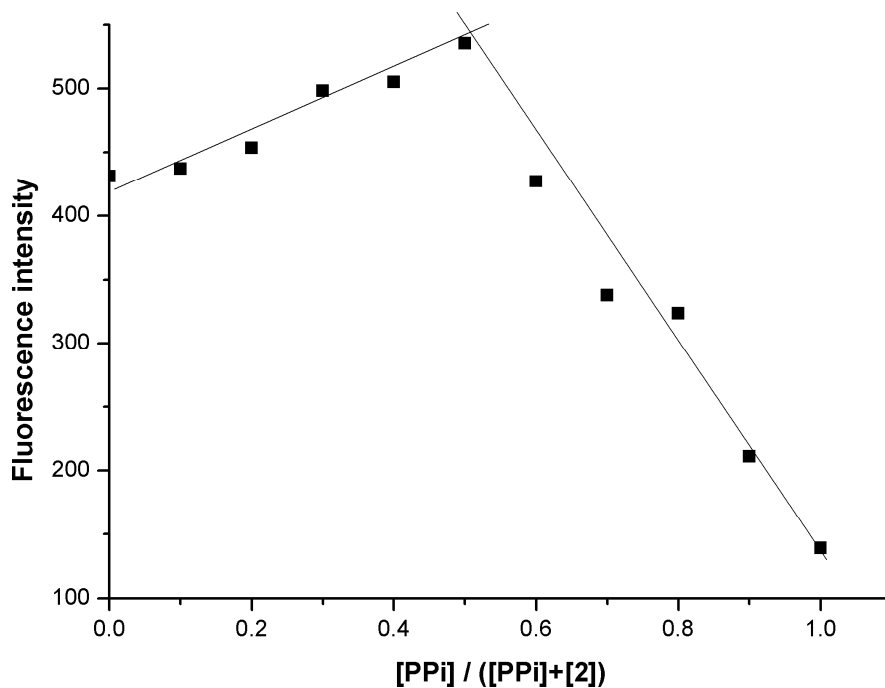


Figure-S8. Job's plot of the complexation between **2** and PPi in 20 mM HEPES solution at pH 7.4. Total concentration of **2** and PPi was kept constant at 3 μ M.

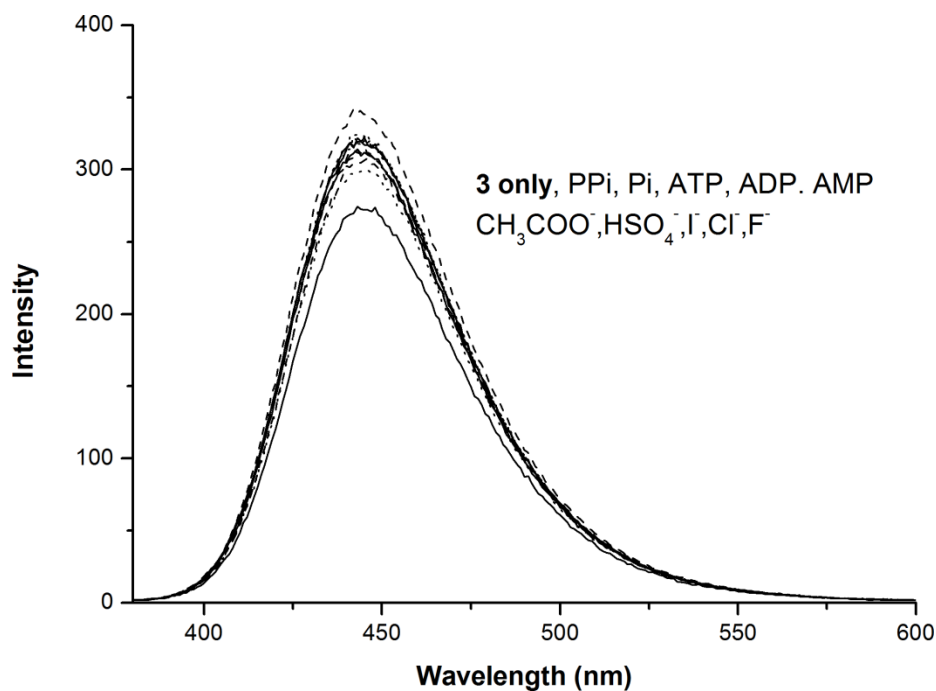


Figure-S9. Plot fluorescence changes of compound **3** (3 μ M) upon the addition of PPi, Pi, ATP, ADP, AMP, CH_3COO^- , HSO_4^- , F^- , Cl^- , Br^- and I^- (100 equiv.) in pH 7.4 (20 mM HEPES) (λ_{ex} = 356 nm, Slit: 1.5 nm/3 nm).

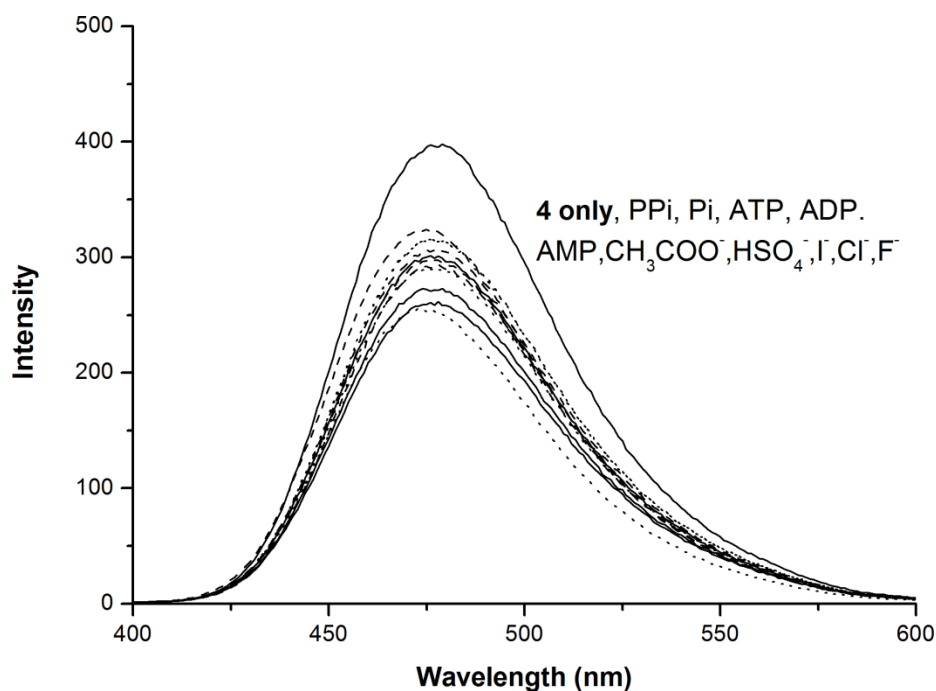


Figure-S10. Plot fluorescence change of compound **4** (3 μM) upon the addition of PPI, Pi, ATP, ADP, AMP, CH₃COO⁻, HSO₄⁻, F⁻, Cl⁻, Br⁻ and I⁻ (100 equiv.) in pH 7.4 (20 mM HEPES) ($\lambda_{\text{ex}} = 379$ nm, Slit: 3 nm/3 nm).

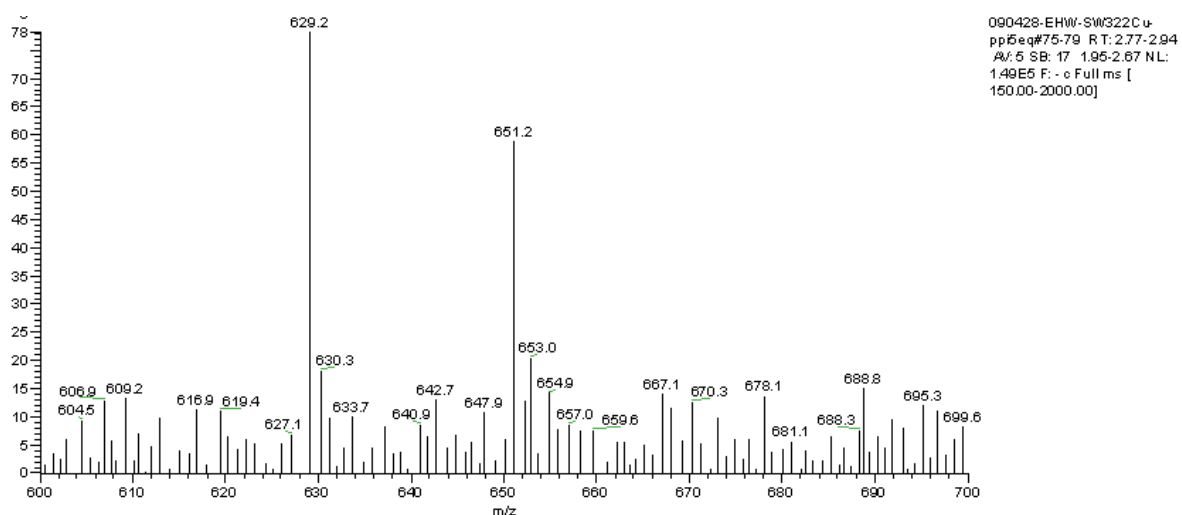


Figure-S11. Portion ESI mass spectrum of **1** upon the addition of excess PPI (5 equiv.).

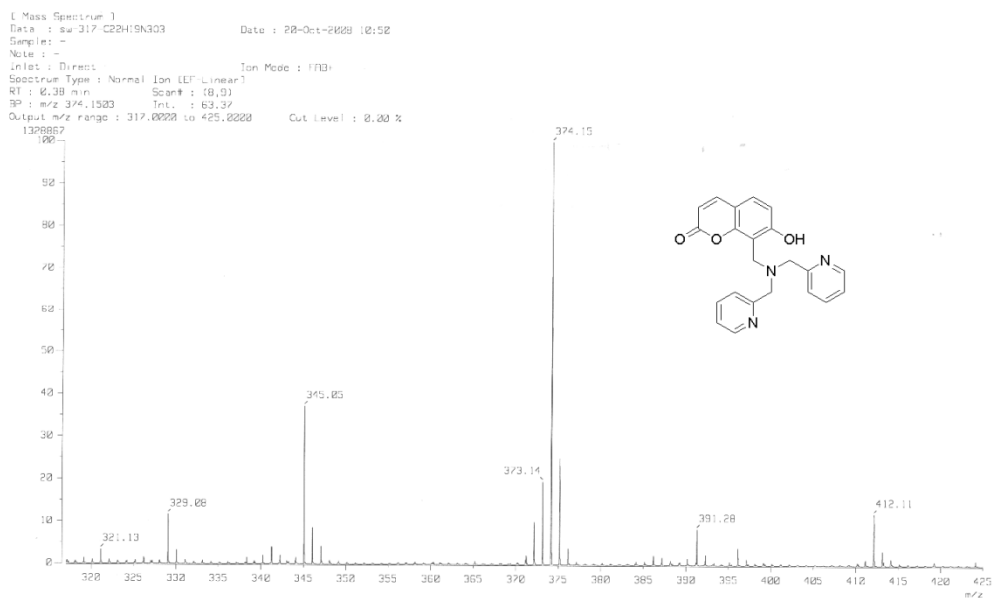


Figure-S14. FAB mass spectrum of compound 5.

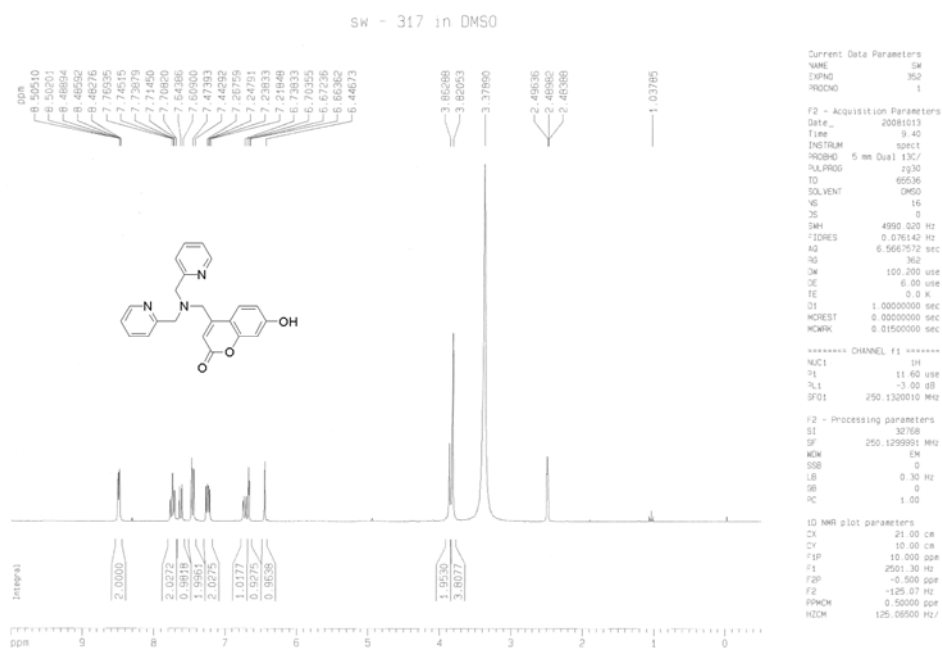


Figure-S15. ¹H-NMR (DMSO-*d*₆, 250 MHz) of compound 7.

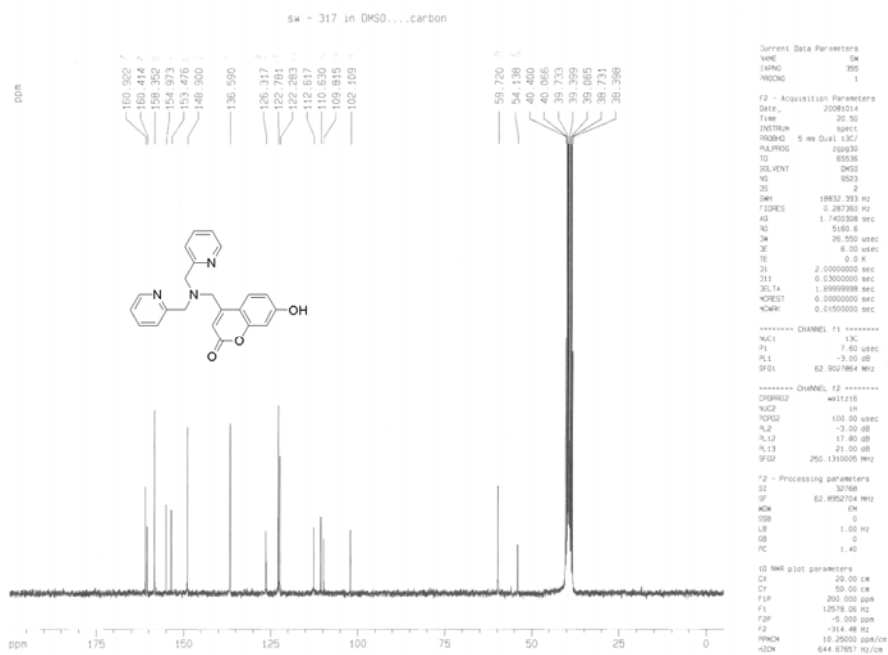


Figure-S16. ^{13}C -NMR (DMSO- d_6 , 250 MHz) of compound 7.

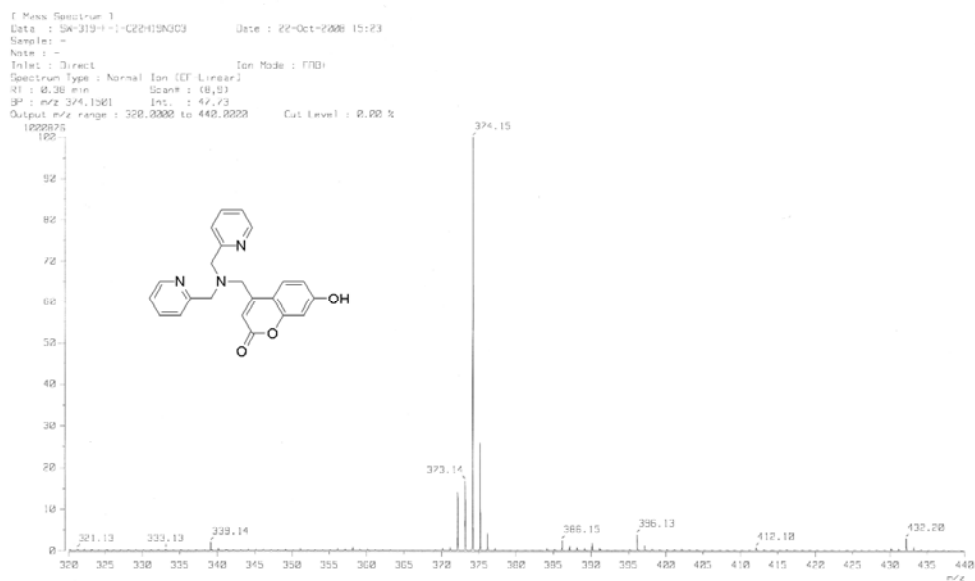


Figure-S17. FAB mass spectrum of compound 7.

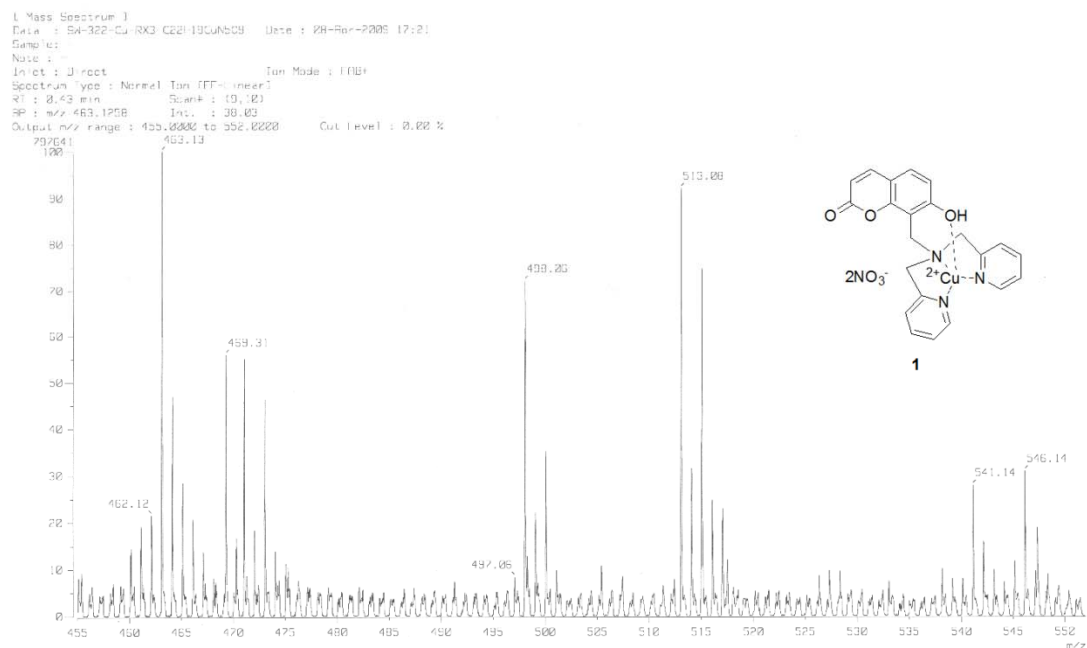


Figure-S18. FAB mass spectrum of compound 1.

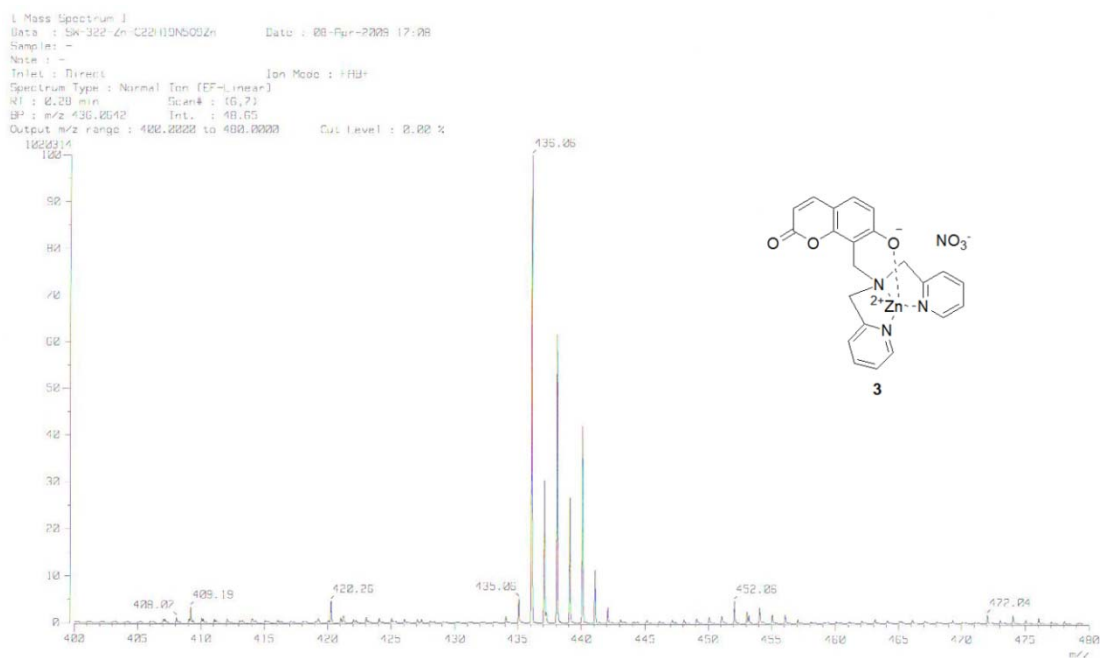


Figure-S19. FAB mass spectrum of compound 3.

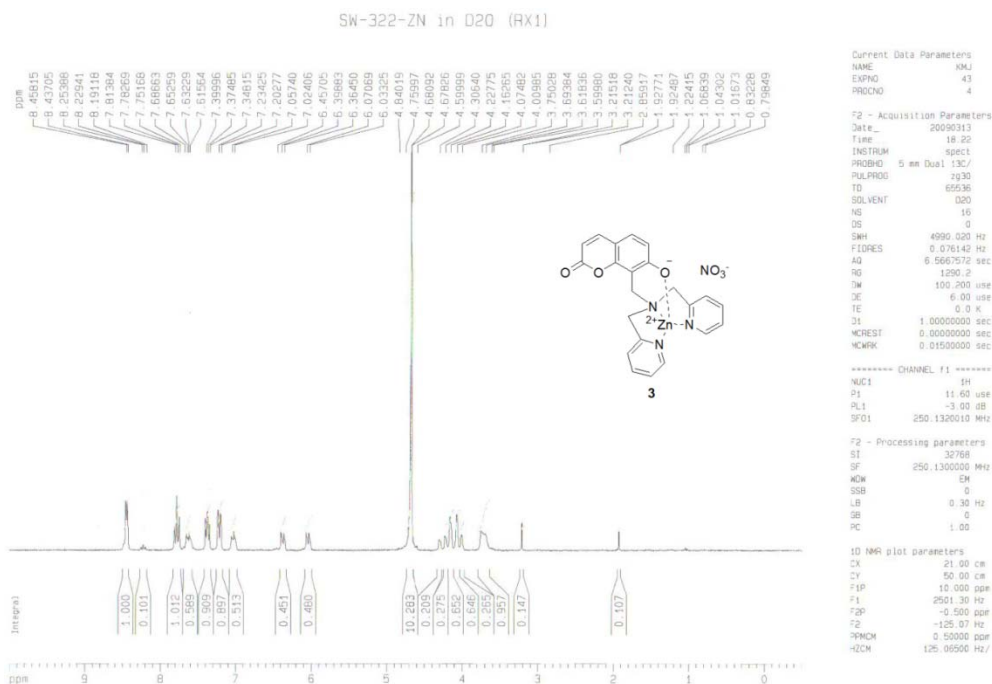


Figure-S20. ¹H-NMR (D₂O, 250 MHz) of compound 3.

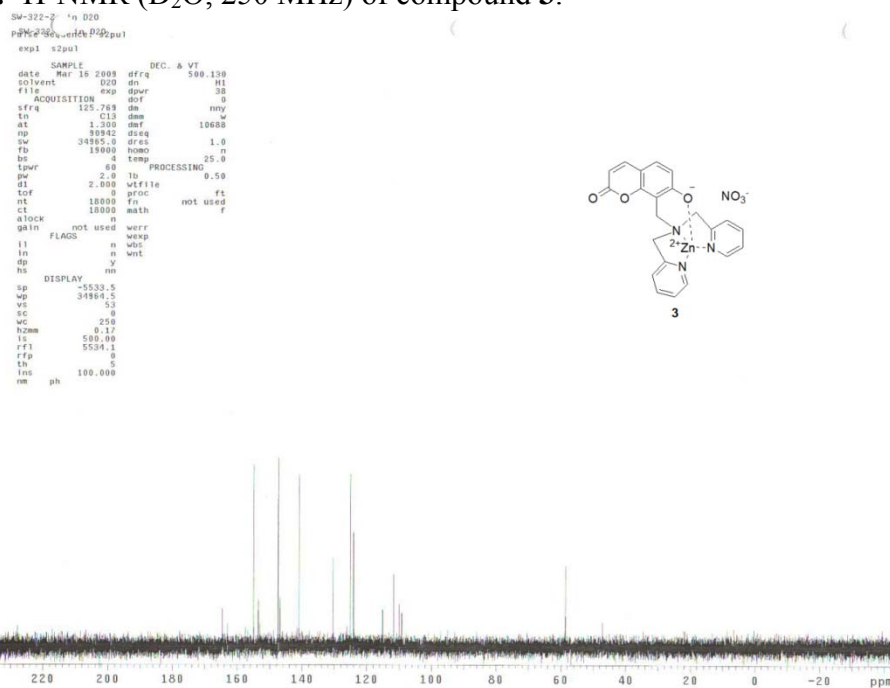


Figure-S21. ¹³C-NMR (D₂O, 250 MHz) of compound 3.

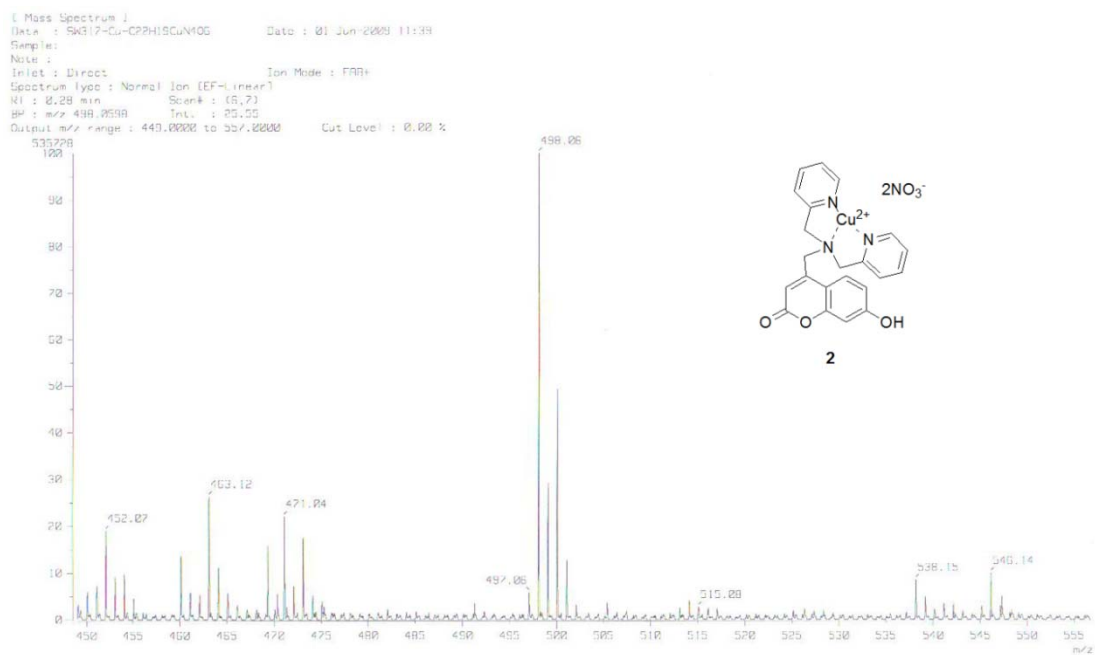


Figure-S22. FAB mass spectrum of compound 2.

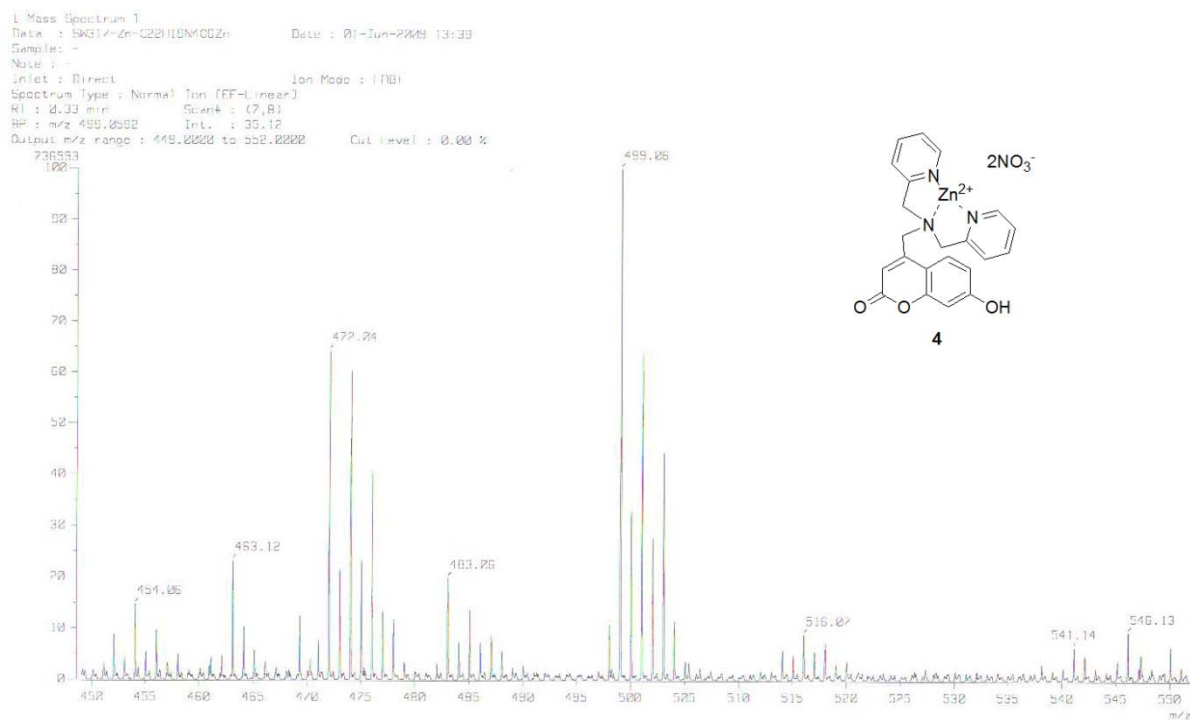


Figure-S23. FAB mass spectrum of compound 4.

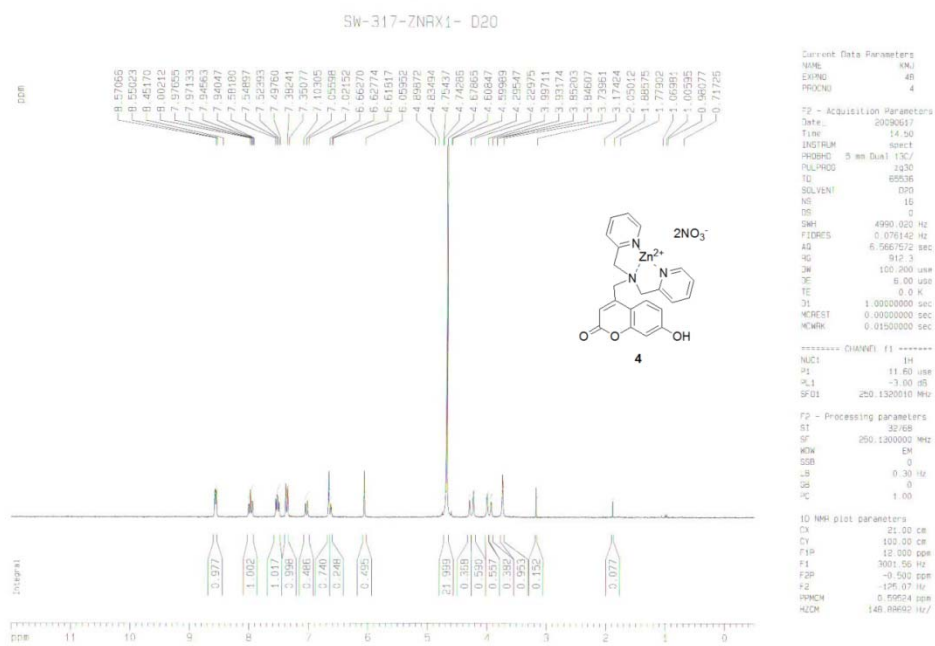


Figure-S24. $^1\text{H-NMR}$ (D_2O , 250 MHz) of compound **4**.

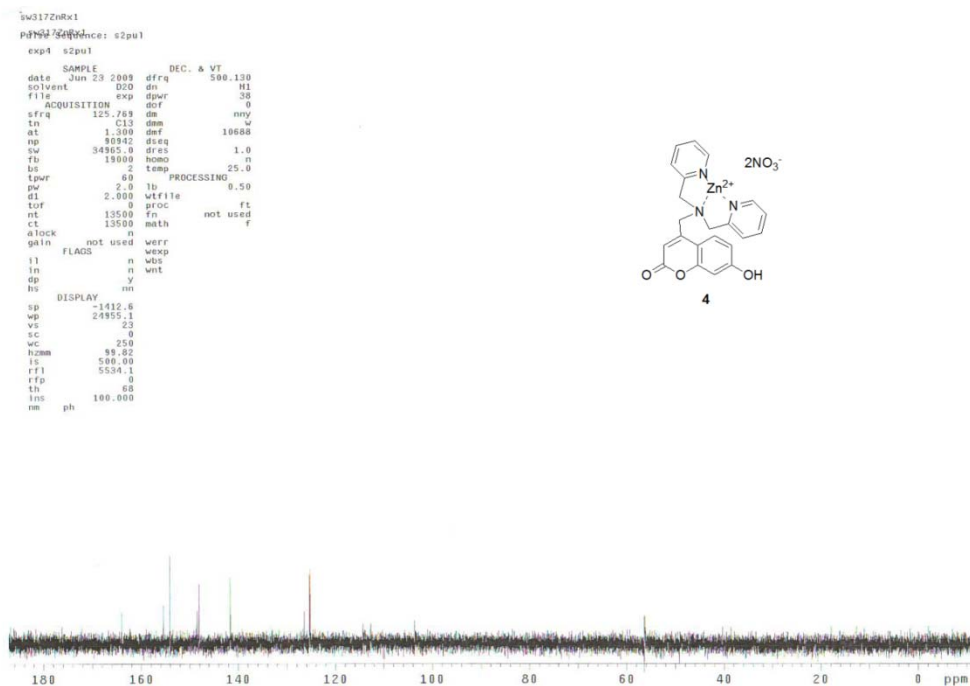


Figure-S25. $^{13}\text{C-NMR}$ (D_2O , 250 MHz) of compound **4**.